NANO LETTERS

XXXX
Vol. xx, No. x
-

Optical Anisotropy in Single-Walled Carbon Nanotube Thin Films: Implications for Transparent and Conducting Electrodes in Organic Photovoltaics

Giovanni Fanchini,* Steve Miller, Bhavin B. Parekh, and Manish Chhowalla

Materials Science and Engineering, Rutgers University, 607 Taylor Road, Piscataway, New Jersey 08854

Received February 25, 2008; Revised Manuscript Received May 21, 2008

ABSTRACT

Optical anisotropy in single-walled carbon nanotube thin film networks is reported. We obtain the real and imaginary parts of the in- (||) and out-of-plane (⊥) complex dielectric functions of the single-walled carbon nanotube (SWNT) thin films by combining transmission measurements at several incidence angles with spectroscopic ellipsometry data on different substrates. In sparse networks, the two components of the real part of the complex dielectric constant ($\varepsilon_{1||}$ and $\varepsilon_{1\perp}$) were found to differ by 1.5 at 2.25 eV photon energy. The resulting angular dependence (from 0 to 70° incidence angles) of transmittance is reflected in the conversion efficiency of organic solar cells utilizing SWNT thin films as the hole conducting electrodes. Our results indicate that, in addition to the transparency and sheet resistance, factors such as the optical anisotropy must be considered for optical devices incorporating SWNT networks.

Low-density networks of single-walled carbon nanotubes (SWNTs) are transparent and conducting.[1–10] The unique optical and electronic properties of SWNT thin films arise from the fact that a fully percolating web can be achieved with less than 1% of the substrate surface being covered by SWNTs.[1,8] Thus, when modeling the optical properties of thin films formed by SWNTs, the variable fraction of voids must be considered. We have shown that[3] the optical constants of the SWNT thin films obtained from the Bruggeman effective medium theory give a reasonably good description of their optoelectronic properties.

Recently, significant work has been devoted toward developing new applications of transparent and conducting SWNT thin film networks. The tunable optoelectronic properties allow transparencies of up to 85% at a sheet resistance of ~50 Ω/□. These optoelectronic properties of SWNT thin films make them ideal replacement for indium tin oxide (ITO) in organic photovoltaics (OPVs),[4–6] organic and inorganic light emitting diodes,[7] displays, touch screens, and smart windows applications. More specifically, the transparent and conducting SWNT thin films are highly flexible and possess a work function that is comparable to ITO, making them ideal as the hole collecting electrodes in OPVs. Indeed, OPVs with SWNT electrodes yield efficiency values that are comparable to ITO (e.g., 2.6% vs 2.8%[5]) on flexible substrates. However, the studies to date have reported OPV characteristics measured under normal illumination, neglecting the possibility of optical anisotropy in SWNT thin films. Similarly, while the optical properties at normal incidence of SWNT thin films have been reported and modeled in detail,[8–11] limited data are available from measurements at lower incidence angles. Our measurements on SWNT thin films at low grazing angles[3] indicate much higher absorbance (i.e., stronger imaginary part of the complex refractive index) than at normal incidence.

Individual carbon nanotubes are indeed known to possess intrinsic optical anisotropy[12,13] due to different optical strengths (σ) of transitions allowed in tangential (ordinary, σ_o) and parallel (extraordinary, σ_e) directions with respect to the tube axes. The fact that the SWNTs in sparse networks are likely to lay flat on the substrate surface should lead to different in- (||) and out-of-plane (⊥) components of the complex dielectric function. Studies suggesting optical anisotropy in SWNT bundles[14] and nanotube−polymer composites[15] have been reported. However, a systematic investigation correlating the effects of the effective optical anisotropy with the amount and distribution of voids in SWNT thin film networks and its impact on the performance of SWNT-based OPVs is lacking.

* Corresponding author, fanchini@rci.rutgers.edu.

10.1021/nl080563p CCC: $40.75
Published on Web 07/22/2008

In this Letter, we describe optical anisotropy of SWNT thin films as a function of their density. Initially, we describe the in- and out-of-plane optical properties which clearly demonstrate anisotropy in SWNT thin films. Subsequently, we correlate the effects of birefringence on the performance as a function of illumination angle of organic solar cells using SWNT networks as the hole-collecting electrodes. We show that the optical anisotropy in SWNT thin film electrodes leads to a variation in efficiency as a function of the angle of illumination in OPVs, in contrast to using ITO electrodes.

The transparent and conducting SWNT (HiPCO) thin films (10−80 mL at 2 mg/L) were prepared by vacuum filtration from aqueous suspensions using the method described in refs 3, 9, and 16. One substantial advantage of the filtration method that we have exploited in our work is that it allows the deposition of SWNT thin films having the same properties on different substrates.[16] The OPVs were assembled on the top of SWNT thin films by spin coating ∼200 nm of regioregular poly(3-hexylthiophene) (P3HT) and phenyl-C_{61}-butyric acid methyl ester (PCBM) (P3HT:PCBM = 1:1) and thermally evaporating aluminum electrodes on top. The details of OPV device fabrication are described in ref 4. For efficiency measurements at varying incidence angles, the device holder was mounted on a precision goniometer.

In general, determination of the optical constants from thin films requires knowledge of the optical constants of the substrate and the measurement of two complementary optical properties. Complementary optical properties can be the reflectance (R) and transmittance (T) of unpolarized light[17] or the ellipsometric angles (Ψ and Δ) related to the change in state of polarization upon light interaction with the sample.[17] Detection of optical anisotropy is customarily achieved by measuring optical properties at varying angles of incidence. However, this is challenging for SWNT thin films because of the poor reflectance of the nanotubes. In addition, such a method is generally limited by accurate calibration of optical instruments,[17] which becomes troublesome for very thin films, especially in reflectance. An alternative method, first proposed by Strachan[18] (described in detail in Supporting Information) has been proven to be effective for discontinuous films or monolayers.[19]

In order to demonstrate optical anisotropy in the films, we performed phase-modulated ellipsometry measurements (Jobin-Yvon UVISEL spectroscopic ellipsometer) at an angle of incidence of 70° on the same film after its deposition on optical-grade glass (Fisher BK7) and (100) silicon substrates. The uncertainty in the procedure (due to roughness and other variations) was estimated by means of measurements on the film laying on the ester membrane used for vacuum filtration deposition of the SWNT thin films (see refs 3, 9, and 16 for details). The ellipsometry data on the different substrates were then simulated using the Jobin-Yvon PsiDelta software by means of anisotropic and isotropic models (see Supporting Information). In order to consider the discontinuous character of our SWNT thin films and the presence of voids, the effective dielectric functions of the SWNT thin films ($\varepsilon_{\mathrm{eff},\parallel}$ and $\varepsilon_{\mathrm{eff},\perp}$, or $\varepsilon_{\mathrm{eff}}$) were determined for both cases from the dielectric responses of the SWNTs ($\varepsilon_{\parallel}$ and $\varepsilon_{\perp}$, or ε) within

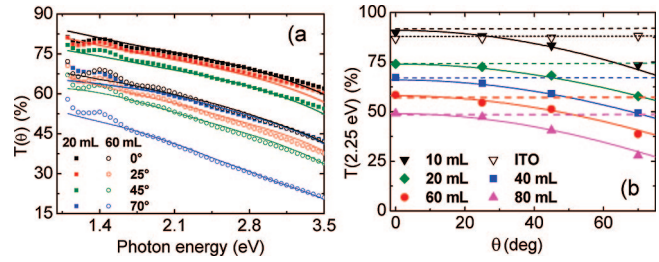

Figure 1. (a) Transmittance of ITO and SWNT films on glass as a function of the photon energy (E) at four incidence angles θ = 0°, 25°, 45°, 75°. (b) Angular dependence of the transmittance for ITO and SWNT films at $E \approx 2.25$ eV showing cosine θ dependence for SWNT films and independence of θ for ITO. Continuous lines represent fits by means of the anisotropic model while dotted lines represent unsatisfactory fits by means of the isotropic model.

the Bruggeman effective medium theory.[20] The SWNT thin films were modeled as being composed of a volume fraction (f) of SWNTs and a complementary fraction ($1 - f$) of voids.

The effective dielectric functions estimated by means of anisotropic and isotropic ellipsometry models were then used to calculate the transmittance $T(\varepsilon_{\mathrm{eff}},\varepsilon_{0\mathrm{glass}},\theta,E)$ of the SWNT films on glass substrates at four incidence angles (θ = 0, 25, 45, and 70°). The calculated transmittance values were then compared with the experimental data measured using a double-beam spectrophotometer (Perkin-Elmer λ20). The experimental and calculated optical properties of SWNT networks of different densities are shown in Figure 1. Specifically, in Figure 1a, the transmittances of two films with very different densities (20 and 60 mL) are shown. It is found that the transmittance values ($\theta = 0-70°$) decrease approximately with the incidence angle according to the cosine law:

$$T_{\mathrm{SWNT}}(E,\theta) \approx T_{\mathrm{SWNT}}(E,\theta{=}0) \cdot \cos(K \cdot \theta) \qquad (1)$$

with $K \approx 0.6$ rad^{-1} at $E \approx 2.25$ eV across the entire visible spectrum. In contrast, Figure 1b shows that the corresponding transmittance of a 100 nm thick ITO layer on glass is virtually independent of θ (i.e., $T_{\mathrm{ITO}}(E,\theta) \approx T_{\mathrm{ITO}}(E,\theta{=}0)$. This happens despite the fact that the 10 mL SWNT thin film has almost the same thickness as ITO, they are both deposited on the same substrate, and the refractive index of ITO (1.7−1.8 at $E = 2.25$ eV) is similar to the 10 mL SWNT film at normal incidence. (See Supporting Information.)

The angular dependence of transmittance in thin film−substrate systems can be rather complicated. However, since our samples (ITO on glass and SWNTs on glass) have similar thicknesses and similar optical properties at normal incidence, the increasingly different behavior with θ is a strong indication that one of the two is experiencing a strong change in complex refractive index (and hence the complex dielectric function). In other words, it is showing anisotropic optical behavior. In Figure 1b, the fits from the two models for the transmittance data at $E = 2.25$ eV are shown. It can be seen that the solid lines (representing the anisotropic model) describe the data much better than the dotted lines (calculated assuming an isotropic material).

Effective complex dielectric functions of SWNT thin films of increasing tube density (filtrate volume 20−80 mL) are

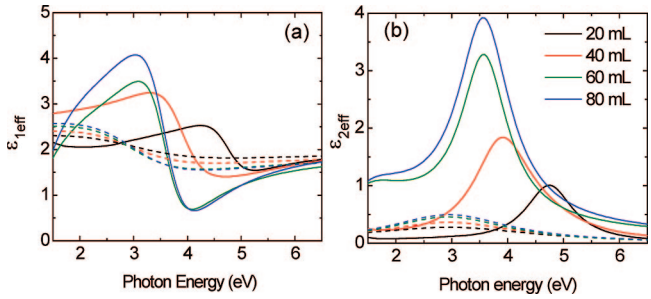

Figure 2. Effective (a) real and (b) imaginary complex dielectric functions of SWNT films extracted by fitting the ellipsometry data using the anisotropic model and the effective medium theory. The lowest values of ε_2 at the lowest tube density (i.e., 20 mL) are a consequence of the higher fraction of voids in these films. Solid and dotted lines represent in- (||) and out-of-plane (⊥) dielectric functions, respectively.

shown in Figure 2, panel a (real) and panel b (imaginary). Increase in absorption suggested by $\varepsilon_{2\text{eff}||}$ and $\varepsilon_{2\text{eff}\perp}$ features expectedly indicates that the number of tubes per unit volume in the films increases as a function of the filtrated volume of SWNT suspension. In addition, if changes in the optical properties are completely due to increase in thicknesses at a constant SWNT density, similar dielectric functions would be expected for the 20 and 80 mL films, in clear contradiction with Figure 2. Furthermore, the maximum intensity of $\varepsilon_{2\text{eff}||}$ (solid lines in Figure 2) almost quadruples from 20 to 80 mL suggesting an approximately linear increase in the fraction of substrate area covered with SWNTs, in agreement with our previous microscopy observations.[3,9] In contrast, the maximum intensity of $\varepsilon_{2\text{eff}\perp}$ (dotted lines in Figure 2) for the 80 mL film is only twice that of the 20 mL film which indicates a sublinear increase in the areal density of tubes in the *xz* and *yz* cross-sectional planes, corroborating the concomitant increase in film thickness by a factor of ~1.5 predicted by data fitting.

Another interesting consideration arising from Figure 2 is that the effective birefringence of our SWNT films ($\varepsilon_{1\text{eff}||} - \varepsilon_{1\text{eff},\perp} \approx -0.2$ to 1.5 for the 20−80 mL films at ~2 eV) is strongly film-dependent and substantially different from that previously reported for individual HiPCO SWNTs ($\varepsilon_{1e} - \varepsilon_{1o} \approx 1.99$[14,15]). Also the absolute values of $\varepsilon_{1\text{eff}}$ are expectedly different from those of individual SWNTs. All these facts point to the importance of considering anisotropically distributed voids along the basal (*xy*) and cross-sectional (*xy* or *yz*) surfaces in order to determine the effective dielectric functions of the SWNT films. That is, the surface fraction covered by SWNTs along the cross-sectional planes is relatively high (40−85%) while it is considerably lower (~1%) along the basal plane, requiring the use of anisotropic effective medium theories for accurately determining the optical constants of SWNT thin films. The physical reasons leading to anisotropy in SWNT thin films are discussed in the Supporting Information.

In order to demonstrate the consequence of optical anisotropy for devices, we correlated it to OPV performance by measuring the efficiency at different angles (θ). We investigated two devices, one with a 100 nm thick ITO film and one with a SWNT network as the hole collecting

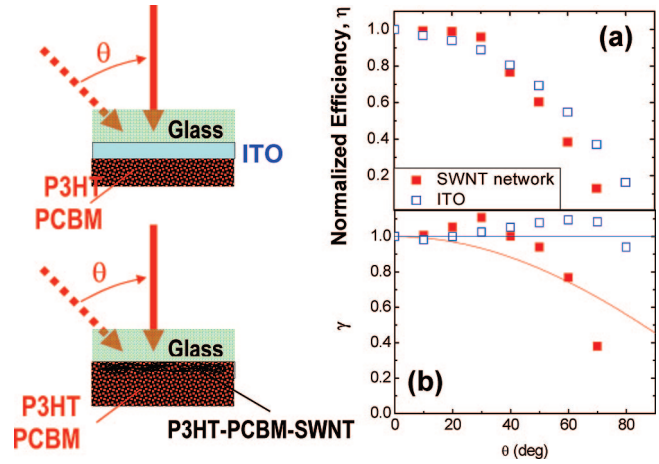

Figure 3. Schematics of solar cells with ITO (top) and SWNT thin film (bottom) as transparent electrodes are shown on the left. The angular dependence of their efficiencies plotted as (a) η, the normalized efficiency, and (b) $\gamma = \eta/(\eta_0 \cos\theta)$. The line fits based on the cosine relationship shown in (b) demonstrate optical anisotropy in SWNT thin film devices and θ independence in ITO ones.

electrodes. The normalized efficiencies (η, taken as the maximum efficiency obtained at a given angle divided by the maximum obtained at normal incidence) of the two devices as a function of θ are plotted in Figure 3a. The use of normalized efficiencies versus the actual values allows comparison of the two different types of devices at various angles. Decrease in efficiency with the angle of incidence can be seen for both electrodes. However, when the system is considered as a whole, the optical anisotropy in SWNT thin films becomes clear. That is, the amount of light illuminating the P3HT:PCBM active layer depends on the transmittance (*T*) of the electrode, composed of the supporting glass substrate and the hole-collecting thin film, as shown schematically in Figure 3. In the framework of a thick film approximation, η can be expressed as

$$\eta(\theta) \sim T(\theta) \approx [1 - R(\theta)] \cdot \exp[-\alpha(\theta)d] \qquad (2)$$

Since P3HT has a much higher refractive index than both glass and ITO, the angular dependence of reflectance (*R*) is mainly due to the P3HT−ITO interface (for ITO electrodes) or by the P3HT−glass interface (for SWNT network electrodes, which exhibit a poor reflectance due to roughness and light scattering). Thus, for both interfaces $R(\theta) \approx 1 - \cos(\theta)$ at $\theta \approx 0-70°$.

Therefore, defining η_0 as the efficiency at normal incidence, the quantity $\gamma = \eta(\theta)/\eta_0/\cos(\theta)$ has approximately the same angular dependence as $\exp[-\alpha(\theta)d]$, where α is the extinction coefficient of the electrode and *d* its thickness. Since α depends only on the extinction coefficient $k = \text{Im}(\varepsilon^{1/2})$, any angular dependence of γ reflects the angular dependence of $\varepsilon(\theta)$ and is indicative of the anisotropy of the transparent, hole-collecting electrode. Indeed, as shown in Figure 3b, γ is almost independent of θ for the OPV using an ITO electrode, while $\gamma \approx \cos(K \cdot \theta)$ (with *K* defined by eq 1) for the SWNT-based solar cells. This is the consequence of the fact that in SWNT thin films ε_2 increases with θ because at visible photon energies, $\varepsilon_{||} > \varepsilon_\perp$.

In conclusion, we have studied the optical anisotropy in transparent and conducting SWNT thin films. We have demonstrated that a realistic model accounting for the experimental data must consider the optical anisotropy of individual SWNTs, their orientation parallel to the substrate, and the role of disorder in releasing the selection rules governing the optical transitions. Finally, we have shown that the different properties of SWNT (anisotropic) and ITO (isotropic) thin films lead to different behavior in the angular conversion efficiency of organic solar cells.

Supporting Information Available: Description of the ellipsometry model used: *n_and_k_of_ITO.jpg* [optical constants of ITO as determined by our "isotropic" method (eq 3b)], *jdosswntfilm0.m* (Matlab routine used to determine the optical properties of SWNT thin films, runs under Matlab 6.5 Release 13 and more recent versions), and *Hipco_n_m.txt*, a list of the (*n*, *m*) indices for Hipco SWNTs as used in our theoretical determination of the optical properties of SWNT thin films. This material is available free of charge via the Internet at http://pubs.acs.org.

References

(1) Hu, L.; Hecht, D. S.; Grüner, G. *Nano Lett.* **2004**, *4*, 2513.
(2) Saran, N.; Parikh, K.; Suh, D.-S.; Muñoz, E.; Kolla, H.; Manohar, S. K. *J. Am. Chem. Soc.* **2004**, *126*, 4462.
(3) Fanchini, G.; Unalan, H. E.; Chhowalla, M. *Appl. Phys. Lett.* **2006**, *88*, 191919.
(4) Du Pasquier, A.; Unalan, H. E.; Kanwal, A.; Miller, S.; Chhowalla, M. *Appl. Phys. Lett.* **2005**, *87*, 203511.
(5) Rowell, M. W.; Topinka, M. A.; McGehee, M. D.; Prall, H.-J.; Dennier, G.; Sariciftci, N. S.; Hu, L.; Gruner, G. *Appl. Phys. Lett.* **2006**, *88*, 233506.
(6) Sgoba, V.; Guldi, D. M. *J. Mater. Chem.* **2008**, *18*, 153.
(7) Aguirre, C. M.; Auvray, S.; Pigeon, S. *Appl. Phys. Lett.* **2006**, *88*, 183104.
(8) Borondics, F.; Kamarás, K.; Nikolou, M.; Tanner, D. B.; Chen, Z. H.; Rinzler, A. G. *Phys. Rev. B* **2006**, *74*, 045431.
(9) Unalan, H. E.; Fanchini, G.; Kanwal, A.; Du Pasquier, A.; Chhowalla, M. *Nano Lett.* **2006**, *6*, 677.
(10) Zhang, D.; Ryu, K.; Liu, X.; Polikarpov, E.; Ly, J.; Tompson, M. E.; Zhou, C. *Nano Lett.* **2006**, *6*, 1880.
(11) Parekh, B. B.; Fanchini, G.; Eda, G.; Chhowalla, M. *Appl. Phys. Lett.* **2007**, *90*, 121913.
(12) de Heer, W. A.; Bacsa, W. S.; Châtelain, W. A.; Gerfin, T.; Humphrey-Baker, R.; Forro, L.; Ugarte, D. *Science* **1994**, *268*, 845.
(13) Tasaki, S.; Maekawa, K.; Yamabe, T. *Phys. Rev. B* **1998**, *57*, 9301.
(14) Fry, D.; Langhorst, B.; Kim, H.; Grulke, E.; Wang, H.; Hobbie, E. K. *Phys. Rev. Lett.* **2005**, *95*, 038304.
(15) Fagan, J. A.; Simpson, J. R.; Landi, B. J.; Richter, L. J.; Mandelbaum, I.; Bajpai, V.; Ho, D. L.; Raffaelle, R.; Hight Walker, A. R.; Bauer, B. J.; Hobbie, E. K. *Phys. Rev. Lett.* **2007**, *98*, 147402.
(16) Wu, Z.; Chen, Z.; Du, X.; Logan, J. M.; Sippel, J.; Nikolou, M.; Kamaras, K.; Reynolds, J. R.; Tanner, D. B.; Hebard, A. F.; Rinzler, A. G. *Science* **2004**, *305*, 1273.
(17) Azzam, R. M. A.; Bashara, N. M. *Ellipsometry and Polarized Light*; North Holland: Amsterdam, 1975.
(18) Strachan, C. S. *Proc. Cambridge Philos. Soc.* **1933**, *29*, 116.
(19) Berreman, D. W. *J. Opt. Soc. Am.* **1970**, *60*, 499.
(20) Bruggeman, D. A. G. *Ann. Phys.* **1935**, *24*, 636.
(21) Fantini, C.; Jorio, A.; Souza, M.; Strano, M. S.; Dresselhaus, M. S.; Pimenta, M. A. *Phys. Rev. Lett.* **2004**, *93*, 147406.
(22) Tauc, J. In *Amorphous and Liquid Semiconductors*; Tauc, J. Ed.; Plenum Press: New York, 1974; pp 173−178.

NL080563P